Atmos. Chem. Phys., 11, 5673–5684, 2011
www.atmos-chem-phys.net/11/5673/2011/
doi:10.5194/acp-11-5673-2011

Atmospheric Chemistry and Physics

Variability and budget of CO_2 in Europe: analysis of the CAATER airborne campaigns – Part 2: Comparison of CO_2 vertical variability and fluxes between observations and a modeling framework

I. Xueref-Remy[1], **P. Bousquet**[1], **C. Carouge**[2], **L. Rivier**[1], **and P. Ciais**[1]

[1]Laboratoire des Sciences du Climat et de l'Environnement, Commissariat à l'Energie Atomique, LSCE-Orme, Orme des Merisiers, 91191 Gif-sur-Yvette CEDEX, France
[2]School of Engineering and Applied, Pierce Hall G3H, Harvard University, Cambridge MA 02138, USA

Received: 11 October 2009 – Published in Atmos. Chem. Phys. Discuss.: 12 February 2010
Revised: 30 July 2010 – Accepted: 24 August 2010 – Published: 20 June 2011

Abstract. Our ability to predict future climate change relies on our understanding of current and future CO_2 fluxes, particularly on a regional scale (100–1000 km). CO_2 regional sources and sinks are still poorly understood. Inverse transport modeling, a method often used to quantify these fluxes, relies on atmospheric CO_2 measurements. One of the main challenges for the transport models used in the inversions is to properly reproduce CO_2 vertical gradients between the boundary layer and the free troposphere, as these gradients impact on the partitioning of the calculated fluxes between the different model regions. Vertical CO_2 profiles are very well suited to assess the performances of the models. In this paper, we conduct a comparison between observed and modeled CO_2 profiles recorded during two CAATER campaigns that occurred in May 2001 and October 2002 over Western Europe, as described in a companion paper. We test different combinations between a global transport model (LMDZt), a mesoscale transport model (CHIMERE), and different sets of biospheric fluxes, all chosen with a diurnal cycle (CASA, SiB2 and ORCHIDEE). The vertical profile comparison shows that: 1) in most cases the influence of the biospheric flux is small but sometimes not negligible, ORCHIDEE giving the best results in the present study; 2) LMDZt is most of the time too diffuse, as it simulates a too high boundary layer height; 3) CHIMERE better reproduces the observed gradients between the boundary layer and the free troposphere, but is sometimes too variable and gives rise to incoherent structures. We conclude there is a need for more vertical profiles to conduct further studies to improve the parameterization of vertical transport in the models used for CO_2 flux inversions.

Furthermore, we use a modeling method to quantify CO_2 fluxes at the regional scale from a chosen observing point, coupling influence functions from the transport model LMDZt (that works quite well at the synoptic scale) with information on the space-time distribution of fluxes. This modeling method is compared to a dual tracer method (the so-called Radon method) for a case study on 25 May 2001 during which simultaneous well-correlated in situ CO_2 and Radon 222 measurements have been collected. Both methods give a similar result: a flux within the Radon 222 method uncertainty (35%), that is an atmospheric CO_2 sink of -4.2 to $-4.4\,\mathrm{gC\,m^{-2}\,day^{-1}}$. We have estimated the uncertainty of the modeling method to be at least 33% on average, and even more for specific individual events. This method allows the determination of the area that contributed to the CO_2 observed concentration. In our case, the observation point located at 1700 m a.s.l. in the north of France, is influenced by an area of $1500\times700\,\mathrm{km^2}$ that covers the Benelux region, part of Germany and western Poland. Furthermore, this method allows deconvolution between the different contributing fluxes. In this case study, the biospheric sink contributes 73% of the total flux, fossil fuel emissions for 27%, the oceanic flux being negligible. However, the uncertainties of the influence function method need to be better assessed. This could be possible by applying it to other cases where the calculated fluxes can be checked independently, for example at tall towers where simultaneous CO_2 and Radon 222

Correspondence to: I. Xueref-Remy
(irene.xueref@lsce.ipsl.fr)

Published by Copernicus Publications on behalf of the European Geosciences Union.

measurements can be conducted. The use of optimized fluxes (from atmospheric inversions) and of mesoscale models for atmospheric transport may also significantly reduce the uncertainties.

1 Introduction

Predictions of future climate change rely on our ability to understand the present and future distribution of CO_2 fluxes (e.g. Geels et al., 2007). However, the value of CO_2 fluxes is still uncertain, especially at the regional scale of 100–1000 km (e.g. Patra et al., 2008; Law et al., 2007; Gurney et al., 2004, 2002). Several methods to quantify CO_2 fluxes exist, mainly inverse modeling (e.g. Rödenbeck et al., 2003; Gloor et al., 2001; Bousquet et al., 1999), the Radon method (e.g. Schmidt et al., 2003, 2001), the boundary layer budget method (e.g. Gibert et al., 2007), and tower flux measurements (e.g. Haszpra et al., 2005). Inverse modeling is the most used approach to quantify regional fluxes, and relies on measurements of atmospheric CO_2 concentrations. Because of the large area they can span in a short time, airborne facilities are a well suited for measuring CO_2 concentrations at the regional scale. In a recent paper, Stephens et al. (2007) highlighted the need to record more vertical profiles for cross-validation of atmospheric transport models. We rely here on airborne in situ CO_2 measurements recorded during two CAATER airborne campaigns conducted on 23–26 May 2001 and 2–3 October 2002 over Western Europe, and during which in situ CO_2 (for both campaigns), CO (CAATER 2 only) and semi-continuous Radon 222 (CAATER 1 only) measurements were collected. In a companion paper (Xueref-Remy et al., 2011), we described the observed atmospheric CO_2 variability. Here, we compare models with observations for the CAATER campaigns. We first assess how a global model and a mesoscale one reproduce CO_2 vertical variability, and second, we use modeled influence functions to quantify CO_2 fluxes during a case study, and assess these results using ^{222}Rn-CO_2 observations in the framework of the so-called "Radon method".

A major source of uncertainty (bias) in atmospheric transport models used in global inversions is how well they represent the variability of CO_2 with altitude (Stephens et al., 2007). Given the range of vertical transport processes (deep convection, boundary layer thermic and dynamical mixing, frontal uplift...) the transport between the atmospheric boundary layer (ABL) and the free troposphere (FT) remains fairly uncertain. This process can be constrained by using CO_2 as a transport tracer and looking at the vertical gradient between the ABL and the FT (Sarrat et al., 2007; Yi et al., 2004; Gerbig et al., 2003a, b; Ramonet et al., 2002). Indeed, the gradient between ABL and FT has an impact on the determination of CO_2 fluxes. As pointed out in Stephens et al. (2007), not only averaged profiles over large regions should be compared, but also profiles at individual sites. Here, we test the influence of the model scale (global and mesoscale) on the reproducibility of the observed vertical variability, but also different land flux models, all chosen with a diurnal cycle as they give better results than models using only monthly means or daily average fluxes (Patra et al., 2008).

Our motivation for the second focus of this paper is that using tools such as influence functions (IF) (e.g. Lauvaux et al., 2009), regional CO_2 fluxes can be constrained. We use here a method to constrain regional to continental fluxes (500–1000 km) directly from observations, coupling influence functions from a transport model and a distribution of fluxes. The model used is LMDZt, which reproduces synoptic transport quite well (Patra et al., 2008). The results of the method are assessed with the independent use of Radon-222, a tracer of known surface fluxes that scales with unknown CO_2 fluxes. We conducted our work on a case study flight of 25 May 2001, during which both atmospheric CO_2 and Radon 222 were simultaneously recorded with no data gap.

In Sect. 2, we provide a comparison between observed and modeled vertical CO_2 profiles for both campaigns. The comparison is done on the CO_2 profile averaged for each campaign, but also for individual profiles. Two transport model (LMDZt, CHIMERE) and three biospheric flux models (CASA, SiB2 and ORCHIDEE) are tested within different combinations. In Sect. 3, we apply the Radon method for inferring CO_2 fluxes, and compare its results with the ones from the modeling method based on influence functions and flux maps. Both methods are compared for the CAATER 1 campaign, during a flight on 25 May 2001.

2 Comparison between observed and modeled CO_2 vertical profiles

We evaluate here vertical transport of CO_2 between the ABL and the FT in the LMDZt and the CHIMERE tracer transport models with vertical profile information from both CAATER campaigns, using land fluxes from CASA, SiB2 and ORCHIDEE for the global model LMDZt and from ORCHIDEE for the mesoscale model CHIMERE. All these models are described here below.

2.1 Model-data comparison set-up

The LMDZt model (Hourdin et al., 2006) is an offline transport model derived from the general atmosphere circulation model of the Laboratoire de Météorologie Dynamique LMDZ (Hourdin and Armengaud, 1999). In this version, LMDZt has a global grid, which is zoomed over Europe at horizontal resolution of 1° by 1°. It is parameterized with a diffusive and thermal turbulence convective boundary-layer scheme, and contains 38 vertical levels up to 3 hPa (between 0 and 4000 m). The transport simulation time-step is 1 h;

horizontal winds are nudged on the ECMWF analyzed fields (Filiberti et al., 2006; Uppala et al., 2005) with a time constant of 3 h, ensuring realistic synoptic CO_2 transport during each campaign (see Peylin et al., 2005; Geels et al., 2007; Patra et al., 2008). For optimal comparison with the CAATER aircraft data, the modeled CO_2 profiles are compared with observation exactly at the same time ($\pm$1 h) and location.

The Eulerian mesoscale chemical transport model MM5-CHIMERE (Schmidt et al., 2001) is a three-dimensional atmospheric transport model primarily designed to make long-term simulations for emission control scenarios on air quality. The model domain used here covers Western Europe at a horizontal resolution of 50 km by 50 km. We use 20 layers in the vertical on terrain following sigma-coordinates, with seven layers in the lowest 300 m and the highest one around mid-troposphere. CHIMERE is an off-line model which requires mass-fluxes for transport calculations. These fluxes are provided by a run of the regional meteorological model MM5 (Grell et al., 1994) with output saved every six hours. MM5 is nudged towards the analyses of the European Centre for Medium Range Weather Forecasting (ECMWF) every six hours. The CHIMERE model is a regional model which consequently requires lateral and top boundary conditions, supplied by a run of the global transport model LMDZ (Law et al., 2008; Hauglustaine et al., 2004) at daily frequency. For further information, see the model server (http://www.lmd.polytechnique.fr/chimere/).

Surface fluxes prescribed globally to LMDZt are: 1) annual fossil fuel emissions from Andres et al. (1996), adjusted to the year of the campaigns. The use of annual emissions for fossil fuel may lead to an underestimate of the variability of simulated CO_2 concentrations (Peylin et al., 2009). Some efforts have been made in past years to produce time-varying fossil fuel inventories for Europe (Pregger et al., 2007). The validation of these products for all European countries is still ongoing and we decided not to use them in our work. 2) Monthly air-sea climatologic fluxes from Takahashi et al. (1999, 2002). And 3) Net Ecosystem Exchange CO_2 flux calculated for each campaign interval, with 3 different flux models: ORCHIDEE, SiB2 and CASA. The ORCHIDEE model (Krinner et al., 2005) simulations were forced by 1/2 hourly meteorological fields interpolated from ECMWF 6-hourly analysis at a resolution of $0.35^\circ \times 0.35^\circ$ for 2001 and 2002. Two other alternative Net Ecosystem Exchange (NEE) hourly flux maps have been prepared (although computed on year 2002 only) for the Transcom-continuous experiment (Law et al., 2008). These alternative NEE flux maps at resolution of $1^\circ \times 1^\circ$ each 3 h, are from SiB-2 (Sellers et al., 1996) and CASA (Randerson et al., 1997) models. It is interesting to use the SIB-2 and CASA data-oriented NEE as an alternative to the ORCHIDEE process-based model NEE, because the phenology of SIB-2 and CASA is driven by satellite greenness index observations during CAATER 2, whereas the one of ORCHIDEE is calculated from climate.

For each campaign, the mean profiles simulated by the chosen model combinations (LMDZt-ORCHIDEE, LMDZt-CASA, LMDZt-SiB2 and CHIMERE-ORCHIDEE) have been computed and compared to the observed mean profile at 100 m vertical resolution (Figs. 1 and 4). Note that as in the companion paper, the altitude has been normalized to the corresponding ABL height for all of the observed and modeled profiles before any averaging step. For each profile, the ABL height has been determined with a precision of $\pm$50 m as the altitude at which the vertical gradient of the potential temperature begins to decrease, and where CO_2 and H_2O present step-changes (Gerbig et al., 2003a). In addition, two typical profiles have been selected among the 14 sampled from each campaign to illustrate the performances of the transport model but also of the flux model on the simulations (Figs. 2 and 5). For each campaign, a correlation plot between the observations and LMDZt or CHIMERE simulations is provided (Figs. 3 and 6) to assess the impact of the transport model scale (global/mesoscale) on the reproduction of the CO_2 gradient between the boundary layer and the free troposphere.

2.2 Results for CAATER-1

On Fig. 1, we can observe that there are only small differences in the mean CO_2 profile between LMDZt coupled to any of the biospheric fluxes, and CHIMERE coupled to ORCHIDEE. We observe that the variability of CHIMERE-ORCHIDEE (2.5 ppm in the PBL, 2.2 ppm in the FT) is higher than from any LMDZt simulation (about 2 ppm in the PBL, 1.2 ppm in the FT). It is lower than the observed variability in the PBL (4 ppm) but higher than the observed variability in the FT (0.5 ppm) (Xueref-Remy et al., 2011). In addition, the mean value of the observed ABL-FT gradient, J, equals 8.9 ppm. The modelled value of J is 2.2 ppm for LMDZt-ORCHIDEE, 1.5 ppm for LMDZt-SiB2, 1.1 ppm for LMDZt-CASA, and 2.3 ppm for CHIMERE-ORCHIDEE (Fig. 1). Thus, the CHIMERE-ORCHIDEE and LMDZt-ORCHIDEE simulations are closer to observations than when using the two other flux models. However, the shape of the averaged profile is not well simulated. None of the model configurations can represent well the decrease of CO_2 observed in the mid-ABL, all being too diffusive.

To illustrate better the role of the transport model scale and of the fluxes, we selected two typical profiles (Fig. 2). The profile on Fig. 2a was recorded around 14:40 UTC on 26 May 2001 in East Germany, north of Oberpfaffenhofen (OBP). The wind was blowing from the west. CO_2 concentration is quite homogeneous in the boundary layer ($\sim$364 ppm), with a minimum higher than during the previous days meaning it is likely that the air has travelled over pollution sources and biospheric sinks whose signals have been mixed by convection (see Fig. 4 in Xueref-Remy et al., 2011). The ABL height is at 2500 m a.s.l., and a marked CO_2 gradient betwen the boundary layer and the free troposphere

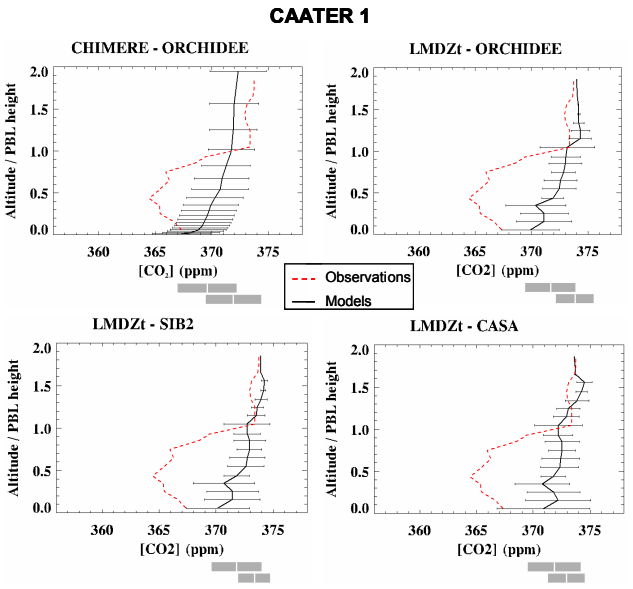

Fig. 1. Comparison of the mean modeled and observed profiles for CAATER 1. Horizontal bars represent the ± 1-σ standard deviation of the mean, computed every 1/10th of the altitude/ABL height ratio. Below the x-axis, the global mean and the ± 1-σ variability in the ABL (upper bar) and FT (lower bar) are shown according to the CO_2 concentration scale given by the x-axis.

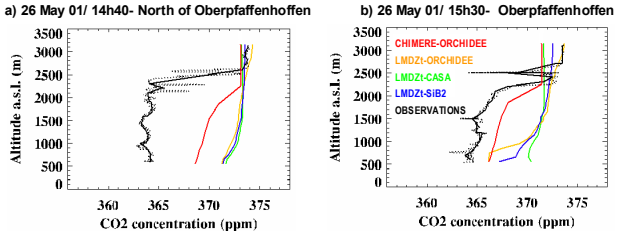

Fig. 2. Comparison between observed and modeled profiles for 2 case studies during the CAATER 1 campaign.

is observed ($J = 9.5$ ppm). The simulations show that: 1) independently of the fluxes, the simulations with LMDZt give a too-smooth profile with a low boundary layer height (around 700 m a.s.l) resulting into a jump J comprised between 1.1 ppm (Sib2, CASA) and 2.1 ppm (ORCHIDEE); and 2) the simulation with CHIMERE-ORCHIDEE is better than LMDZt-ORCHIDEE in terms of shape, although not perfect as it produces a decrease in CO_2 below the top of boundary layer as seen on observations, but also in terms of jump ($\sim$4 ppm). The influence of biospheric fluxes is rather small, indicating that profiles can evaluate transport properties. In addition, the mesoscale model CHIMERE captures the large CO_2 increase across the top of the boundary-layer better than the global model LMDZt.

The profile on Fig. 2b was recorded over OBP around 15:30 UTC on 26 May 2001, with wind blowing from the North. Here as well, the minimum ($\sim$364 ppm) is not as high as during the previous days (see Fig. 4 in Xueref-Remy et al., 2011). The ABL height is located at 2400 m a.s.l. and the cross ABL vertical CO_2 gradient is quite well marked ($J =$ 8.2 ppm). Figure 2b shows that: 1) the LMDZt simulations underestimate the top of the boundary layer ($\sim$900 m a.s.l.) compared to observations but are quite sensitive this time to the surface fluxes, with $J = 1.1$ ppm, 3.5 ppm and 6.2 ppm for CASA, SiB2 and ORCHIDEE, respectively; and 2) the shape of the profile simulated by CHIMERE-ORCHIDEE is more realistic than with LMDZt-ORCHIDEE, with a boundary layer height located at $\sim$2100 m a.s.l. close to the observed value. The simulated gradient $J = 4.1$ ppm with CHIMERE-ORCHIDEE is lower than the observed one and lower than with LMDZt-ORCHIDEE. The LMDZt-ORCHIDEE combination has best performances among the three sets of biospheric fluxes to simulate the observed gradient. The bias of this simulation seems to come from the fact that the boundary layer height is simulated at too low a level. The CHIMERE-ORCHIDEE simulation is the closest to the observations, as the mesoscale model manages to reproduce (even if not strongly enough) the structure of the profile. Whatever the transport model, ORCHIDEE gives the best results among the three biospheric fluxes tested.

Figure 3 provides a model vs. observed scatter plot of J for the 14 profiles of CAATER-1 for the LMDZt-ORCHIDEE and CHIMERE-ORCHIDEE couples (ORCHIDEE being identified as the best NEE model for CAATER-1). The modeled J value of LMDZt-ORCHIDEE is weakly correlated with the observed value (R^2=0.07, slope=0.13) and is also less variable across profiles. Although the sign of the J is correctly modelled for all the profiles, its magnitude is underestimated. This indicates that modeled vertical transport during CAATER-1 is too vigorous in LMDZt. In particular, the ABL height is not marked at all in LMDZt, opposite to the sharp CO_2 discontinuity observed in the aircraft profiles. The CHIMERE-ORCHIDEE simulation of J is not better correlated with the observations ($R^2 = 0.07$, slope $= 0.16$). Analysis of individual profiles (not shown) reveals that CHIMERE tends to do slightly better than LMDZt while understimating J.

2.3 Results for CAATER-2

Figure 4 shows a comparison between observations and model simulations for CAATER-2. As opposed to CAATER-1 (see Fig. 1), here we can observe that the average LMDZt profile is sensitive to the biospheric fluxes, especially near the surface where there is a depletion of CO_2 due to net plant uptake. CHIMERE-ORCHIDEE does not simulate the mean CO_2 vertical profile better than LMDZt. Variability in CHIMERE-ORCHIDEE is higher than in both LMDZt and the observations, as seen by the high standard deviation of the 100 m resolution profile (reaching 9 ppm in the

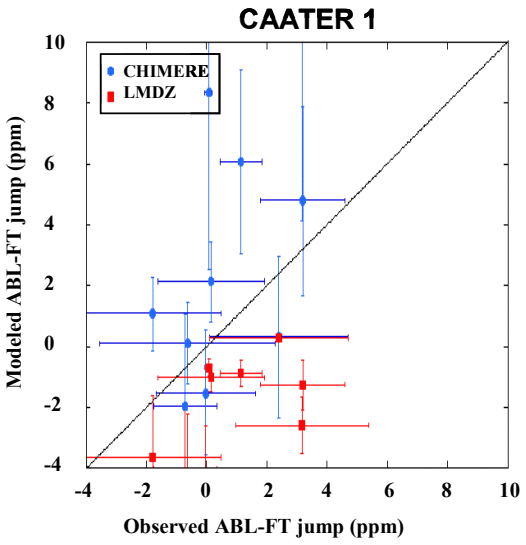

Fig. 3. Comparison of the modelled ABL-FT jumps from LMDZ-ORCHIDEE and CHIMERE-ORCHIDEE to the observed jumps for CAATER 1. Points represent the mean jump for each profile and bars represent the associated ± 1-σ standard deviation.

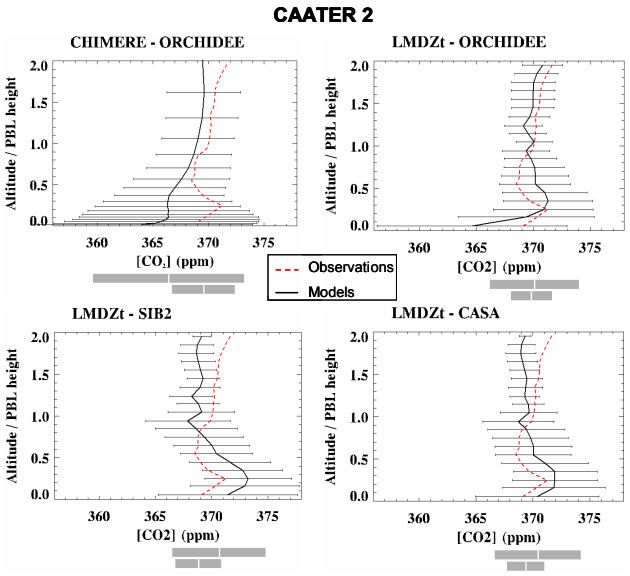

Fig. 4. Comparison of the mean modeled and observed profiles for CAATER 2. Horizontal bars represent the ± 1-σ standard deviation of the mean, computed every 1/10th of the altitude/ABL height ratio. Below the x-axis, the global mean and the ± 1-σ variability in the ABL (upper bar) and FT (lower bar) are shown according to the CO_2 concentration scale given by the x-axis.

lowest levels, compared to an observed value of 4.3 ppm (see Fig. 11 in Xueref-Remy et al., 2011). Furthermore, let us recall the observed ABL-FT gradient, J=+0.8 ppm; compared to J=−0.3 ppm in LMDZt-ORCHIDEE, −1.8 ppm in LMDZt-SiB2, −1.1 ppm in LMDZt-CASA, and 3.2 ppm in CHIMERE-ORCHIDEE (Fig. 4). Thus, all LMDZt simulations give negative values of J, unlike in the observations. By contrast, the CHIMERE-ORCHIDEE simulated J value is positive as is the observed one. However, LMDZt-ORCHIDEE and LMDZt-CASA combinations are best at reproducing the variability observed in the PBL. Even if having opposite signs, the gradient J is small in both cases, as in the observations. The LMDZt-ORCHIDEE can be selected as the best simulation in terms of jump and profile structure, closely followed by the LMDZt-CASA coupling.

Figure 5 shows two typical profiles to evaluate the effect of transport model scale and of NEE. Figure 5a profile has been recorded above the ORL site, at 11:15 UTC on 2 October 2002. A southerly wind was blowing (see Fig. 5 in Xueref-Remy et al., 2011). The ABL top was observed at 750 m a.s.l., and the gradient J was 1.5 ppm. In the ABL, CO_2 varied between 368 ppm and 377 ppm (likely a mixture of vegetation uptake, respiration transport and anthropogenic sources), while it was 372.5 ppm in the free troposphere. All the LMDZt simulations show an accumulation of CO_2 near the ground that is not observed. The model-data misfit is independent of the underpinning NEE flux model, giving a negative $J \approx 3.5$ ppm. Also, the ABL height is too high in the simulation (around 1450 m a.s.l). By contrast, the CHIMERE-ORCHIDEE simulation represents quite well the homogeneous vertical profile in the free troposphere. However, the CO_2 profile in the ABL has an opposite shape to the observed one, the model giving an accumulation of CO_2 near the ground, followed by an inversion of the CO_2 gradient near the observed boundary layer height.

The second case study profile in Fig. 5b was recorded over Thüringen, eastern Germany at 10:00 UTC on 3 October 2002. A west/south-westerly wind was blowing (see Fig. 5 in Xueref-Remy et al., 2011). The ABL height was found at 550 m a.s.l., with a large negative gradient J=−9.1 ppm. The data seem to contain an influence by local pollution in the lowest levels, with a maximum of CO_2 reaching 385 ppm. LMDZt prescribed by ORCHIDEE, SiB2 and CASA NEE give distinct profiles. The three NEE flux models produced a negative ABL-FT gradient (J=−4.5 ppm in SiB2, J=−5.1 ppm in CASA, J=−10.9 ppm in ORCHIDEE) as in the observation. The ABL height is simulated too high as in the previous case (around 1300 m a.s.l. for SiB2 and CASA, and 1500 m a.s.l. for ORCHIDEE). But, indeed, if the ABL height was simulated properly in LMDZt-CASA and LMDZt-ORCHIDEE runs, the CO_2 maximum in the ABL would be about 2.3 higher and would match the observed profile quite well (see inset in Fig. 5b). The CHIMERE-ORCHIDEE simulation leads to a CO_2 profile oscillating around the observations, too variable and with a very small J value making the ABL height hard to define from CO_2. In this case, the parameterization of the model is not diffusive enough.

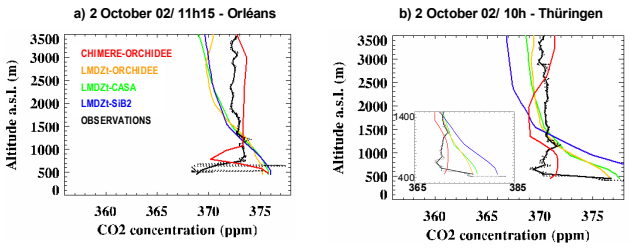

Fig. 5. Comparison between observed and modeled profiles for 2 case studies during the CAATER 2 campaign.

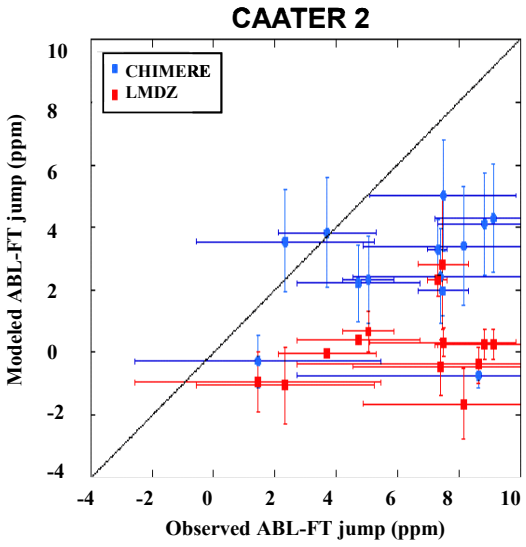

Fig. 6. Comparison of the modelled ABL-FT jumps from LMDZ-ORCHIDEE and CHIMERE-ORCHIDEE to the observed jumps for CAATER 2. Points represent the mean jump for each profile and bars represent the associated ± 1-σ standard deviation from observations and models.

Figure 6 provides a model vs. observed scatter plot of J for LMDZt-ORCHIDEE that we have identified to be the best combination for LMDZt and NEE model in CAATER-2 as for CAATER-1, and for CHIMERE-ORCHIDEE. A similar bias in LMDZt is observed resulting in J values that are too small and not variable enough, as is the case for CAATER-1. However, the model low bias is smaller than for CAATER-1, and the modelled vs. observed linear regression slope of J is better defined (R^2=0.3, slope=0.6) indicating that the model captures different J better. The CHIMERE-ORCHIDEE tends to overestimate the J values with too large a sensitivity (R^2=0.3, slope=1.3).

2.4 Discussion

One finding of this comparison is that the NEE flux magnitude may occasionally play a role in determining the magnitude and the sign of the ABL-FT gradient J, and the shape of the CO_2 vertical profiles (see for instance the profile on Fig. 2b). Among the three NEE models tested, ORCHIDEE (a climate driven model) gives the best results compared to SiB2 and CASA (process-based models); but let us recall that ORCHIDEE has been prepared for both 2001 and 2002, while CASA and SiB2 only for 2002. However, errors in model transport seem to be the most frequent cause of mismatch with observations. This demonstrates that vertical profiles can be used efficiently as a constraint to *falsify* model transport. This was shown for instance by Stephens et al. (2007) for monthly profiles at various sites around the globe, and we here confirm the results of this global study using the two CAATER intensive campaigns. The fact that the value of J differs strongly among the profiles during the same campaign is important to outline, because it suggests that the CAATER airplane trajectory sampled a diversity of flux-transport situations that can be used to cross-validate LMDZt and CHIMERE.

When the LMDZt model global results are contrasted with CAATER-1 data, in the lowermost atmosphere between 0 and 4000 m, the model shows *consistently* the bias of simulating too stiff vertical profiles. This points to an overestimation of the mixing rate between the ABL and the FT. It is possible that the entrainment zone and the non-mixing zone at the top of the ABL are not well resolved by the model parameterization when convection is established (Gibert et al., 2007) (Hourdin et al., 2002). An overestimation of ABL-FT mixing by transport models was already shown by Yi et al. (2004) using CO_2 vertical profiles along the WLEF tall tower in Wisconsin, and by Ramonet et al. (2002) using ABL aircraft vertical profile data during an intensive campaign over a forest in Russia. In CAATER-2, the LMDZt model results show that the boundary layer upper level is systematically too high. It may be noted that the model is unable to reproduce a shallow boundary layer and is too diffusive. At a large scale, the cross-validation analysis of global transport models by Stephens et al. (2007) also pointed to an overestimation of simulated vertical transport in summer, just as we found for the LMDZt model in CAATER-1 and CAATER-2. But the Stephens et al. dataset was more related to evaluation of vertical mixing in the mid troposphere, driven by cloud transport and frontal activity than the CAATER dataset.

The CHIMERE model results including the underlying dynamical fields of MM5 are globally better than those of LMDZt, as the vertical tranport simulated by CHIMERE is less diffusive. Even if not perfect, CHIMERE often improves the representation of vertical structure of the profiles (see for example profiles from Fig. 2). However, the modeled CO_2 profile is too variable at times leading to unrealistic behavior such as seen in Fig. 5b.

Although the mesoscale model CHIMERE appears to be better able to reproduce CO_2 vertical variability than the global model LMDZt, this kind of study should be extended to more data, and more synoptic situations. It underlines the

strong need for more aircraft campaigns to generate vertical profiles to help to calibrate vertical transport parameterization in models and to better constrain CO_2 flux calculation through inverse modeling (Stephens et al., 2007).

3 Regional CO_2 flux calculation

We estimate here regional CO_2 fluxes using two independent methods. The first method, based on collocated CO_2 and Radon 222 observations, is called "the Radon method". The second method combines influence function of the measurement to surface fluxes calculated by LMDZt with an a priori distribution of surface fluxes. Both methods are applied to a case-study during the CAATER-1 campaign and the results are compared to each other.

3.1 Flux calculation with the Radon method

Simultaneous ^{222}Rn and CO_2 concentration observations allow the inference of unknown CO_2 surface fluxes, assuming known ^{222}Rn fluxes within the hypothesis on the ^{222}Rn flux distribution. This dual tracer method, where the concentration change of tracer is scaled to the other in proportion of their surface fluxes, has been applied to ground-based observatories time series (Biraud et al., 2000, 2002; Levin, 1984, 1999; Schmidt et al., 1996, 2001; Wilson et al., 1997). Radon 222 is a radioactive noble gas with a half-time of 3.8 days, that is emitted at relatively constant rates by soils, while the flux from the ocean surfaces is negligible. ^{222}Rn emitted by soils is transported by winds and reduced by radioactive decay. We make the (reasonable) hypothesis that the surface flux of ^{222}Rn is uniform and constant (but we take into account its variability for error calculation, see below) in order to infer less well-known continental emissions of other compounds. According to Schmidt et al. (2001), CO_2 fluxes can be calculated using Eq. (1) below, on condition that the correlation factor between Radon 222 and CO_2 data is better than 0.5 (Levin et al., 1999). The calculated CO_2 fluxes is thus expressed as:

$$j_{CO_2} = j_{Rn} x \Delta C_{CO_2} / \Delta C_{Rn} x [1 + \lambda_{Rn} C_{Rn} / (\Delta C_{Rn} x \Delta t)]^{-1} \quad (1)$$

In Eq. (1), ΔC_{CO_2} and ΔC_{Rn} are the species spatial gradients between the concentration at the measurement location and the marine boundary layer (MBL) concentration, this latter being taken as a baseline, on the day and at the latitude of the measurement; λ_{Rn} is the radioactive half-time of ^{222} Rn (3.814 days), j_{Rn} is the surface ^{222} Rn flux influencing the airborne observation and Δt defines a transit time of air parcel from emission to the observation site. Note that in other papers (e.g. Biraud et al., 2000, 2002; Schmidt et al., 2001, 2003) Δ stands for temporal, not spatial, gradients.

In the following, we first explain the Radon instrumentation and then apply the Radon method to a case study.

3.1.1 Semi-continuous Radon-222 instrumentation

Radon has been measured with the AVIRAD instrument (Filippi, 2000), which consists of an isokinetic probe fixed to the fuselage and of a filtration unit located inside, with limited and straight tubing between the probe and the filter. The isokinetic probe was built by Sextant Avionique Corporation using the same design as for the NASA C-141 (Kritz et al., 1998). The radon measurements are made with alpha spectrometry of the radon progeny products deposited on the collected aerosols. The Paper Filtering Unit is provided with 4 Si detectors in order to measure the alpha activity of each sample at 4 successive decay times. The Data Acquisition System runs 4 alpha spectrometers allowing implementation of different methodologies to validate the radon concentration data. The probe includes a stagnation reservoir, the null-type air inlet and a flow line sensor. It was mounted on the cargo window, under the airplane. At the location of the probe, the boundary layer of the plane was expected to be less than 10 cm. Thus in order to keep the air inlet beyond the boundary layer of the plane, it was fixed at the tip of a 29-cm long mast. The null-type nozzle operates by measuring static pressure on the outside of the probe nozzle, and static pressure inside the inlet opening of the nozzle. When zero pressure differential is developed between the inside and outside pressure taps, the isokinetic velocity is obtained. This null differential pressure is automatically adjusted in real-time. The null-type nozzle was calibrated in a wind tunnel for the Mach number range of the aircraft, between Mach number 0.6 and 0.7. At the rear part of the air inlet, a flow-line sensor made of 4 dynamic pressure taps is used during test flights to make sure that the angle of attack of the isokinetic nozzle was as close as possible to zero. The flow line sensor was also calibrated in a wind tunnel for the Mach number range of the aircraft. Except during turns and turbulences, the angle of attack of the probe was less than 2 degrees, even during ascents and descents. The Filter Unit used a continuous paper filter strip which is advanced by a motorised take-up spool at programmable time intervals. To preserve the collected samples, a blank strip is rolled up along with the filtering strip on the take-up spool. Different paper filter media can be used depending on subsequent analytical procedure. The number of samples per spool is about 70. The active area of each sample is 1700 mm^2. The precision of the measurement is 30%.

3.1.2 Case study

The uncertainties associated with Eq. (1) are the following. First, we suppose a constant and uniform ^{222}Rn flux. In reality this flux depends on soil bedrock type, total pore space, tortuosity, soil moisture and precipitation. Its mean variability in Western Europe soils is of the order of 30% (Nazaroff, 1992; Jutzi, 2001; Ielsch et al., 2002; Szegvary et al., 2007). Secondly, the ^{222}Rn measurement precision itself is $\sim$30%

which translates into a relative error of the same magnitude in the inferred CO_2 surface flux. Thirdly, the error on the transit time is of the order of 6 h, that is a 5% error on the inferred CO_2 flux. In total, we estimate the error on the CO_2 flux of Eq. (1) to be 35%. This is similar to the uncertainty estimated in Schmidt et al. (2003).

3.2 Flux calculation using influence functions and map fluxes

Although back-trajectories are useful tools to trace the origin of air masses, they do not allow a quantitative determination of the influence of surface flux on the atmospheric CO_2 concentration. Here, we use influence functions (IF) calculated by backward transport in the LMDZt model (Hourdin et al., 2006) to quantitatively link surface fluxes and aircraft-measured concentrations. Briefly, a mass of inert tracer is emitted at each aircraft measurement location and transported backward in time using the LMDZt 3-D dynamical fields, backward transport being an analog of the adjoint of the transport. This resulting influence function (IF) to surface fluxes quantifies the contribution of each surface grid point to a given measurement. The IF is the potentital sensitivity of the measured concentration to surface fluxes (e.g. Lauvaux et al., 2009; Krol et al., 2003; Stohl et al., 1998a, b, c). Indeed, even if the vertical transport parameterizations have shown some weaknesses in global transport models such as LMDZ, synoptic transport in LMDZt is proven to be quite well-represented (Patra et al., 2008). We combined IF, as calculated by LMDZt, with surface flux maps in order to estimate CO_2 fluxes influencing the airborne observations, assuming that the flux model is already a realistic image of the flux. IF are computed for five days backwards (corresponding to the Δt from Sect. 3.1) at the observing point corresponding to event D in Fig. 7a, starting at noon, which is the time when the depletion of CO_2 started to occur. Note that on Fig. 8a, IF are only shown for days 1–3 backwards, as for days 4–5, the signals are less than 1% of the maximum sensitivity. The surface flux (Fig. 8b) is the sum of a priori fluxes described in Sect. 2: air-sea flux from Takahashi et al. (1999, 2002), fossil fuel emissions from Andres et al. (1996) and NEE from ORCHIDEE (Krinner et al., 2005) as this was the model that gave the best results among the 3 biospheric models tested in Sect. 2. By multiplying the IF by this a priori flux map, we infer the CO_2 flux (Fig. 8c) which influences the airborne observations to be $-4.39\,\mathrm{gC\,m^{-2}\,day^{-1}}$. NEE contributes dominantly for 73.2% of the total flux as a sink ($-6.91\,\mathrm{gC\,m^{-2}\,day^{-1}}$), fossil fuel emissions for 26.8% as a source ($+2.53\,\mathrm{gC\,m^{-2}\,day^{-1}}$). The ocean contribution is a sink less than 0.01% of the total flux.

Although LMDZt has been proven to model transport at the synoptic scale quite well, the dynamics are not perfect (Patra et al., 2008; Geels et al., 2007). Furthermore, the method here relies on a flux set that has not been optimized. Thus, there are two sources of errors in the method: transport

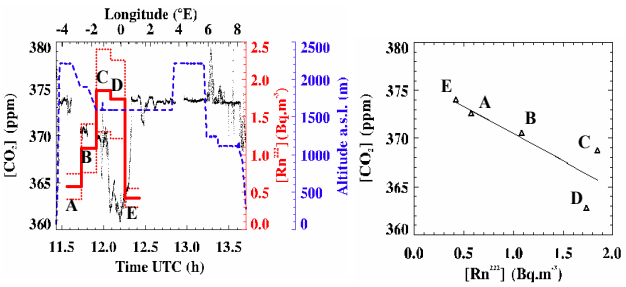

Fig. 7. Left panel: Radon concentration (red plain line) with measurement precision (red dashed line), CO_2 concentration (black plain line) and altitude (blue dashed line) concentrations vs. time measured during CAATER 1 on 25 May 2001. The longitude is indicated on top. Jumps in Radon and CO_2 concentrations are defined as events A to E. Right panel: CO_2 vs. Radon 222 concentration for events A to E.

uncertainties and flux veracity. Indeed, the method allows an estimation of the flux distribution that influences the observations, rather than a real optimization of the flux. Assessing the differences between observed and modeled CO_2 concentrations, we can attempt a rough estimate of the error in the method. Figure 9 represents a comparison between the time-series of the observed CO_2 concentration along the aircraft path, and altitude/time cross sections of the LMDZt/flux set simulation. Three main points can be highlighted:

1. The simulation represents mainly two air masses in the PBL: one during the first half of the flight, with concentrations in the range of 368–370 ppm typically representative of a mixture of oceanic and biospheric air lower than the marine boundary layer (MBL) background value (374.5 ppm: see Xueref-Remy et al., 2011). And a second one during the second half of the flight, with higher concentrations of about 373 ppm close to the MBL background concentration typical of oceanic air-masses, with some peaks at 380 ppm indicating an enrichment of air masses in CO_2 due to fossil fuel emissions from the Benelux and the Ruhr regions. This is in agreement with the back-trajectories analysis conducted in the companion paper (Xueref-Remy et al., 2011).

2. The match between the median amplitudes (and not the mean ones!) of the observed concentrations and the modeled ones is quite good, with an observed median amplitude of about 6 ppm versus a simulated median amplitude of about 4 ppm. This leads to an underestimation of about 33% by the model framework.

3. The model framework does not reproduce concentration extremes such as the observation depletion during the Radon episode D around 12:10 UTC, and the peak of CO_2 of 380 ppm observed over the Ruhr area around 13:15 UTC. The amplitude between extremes is

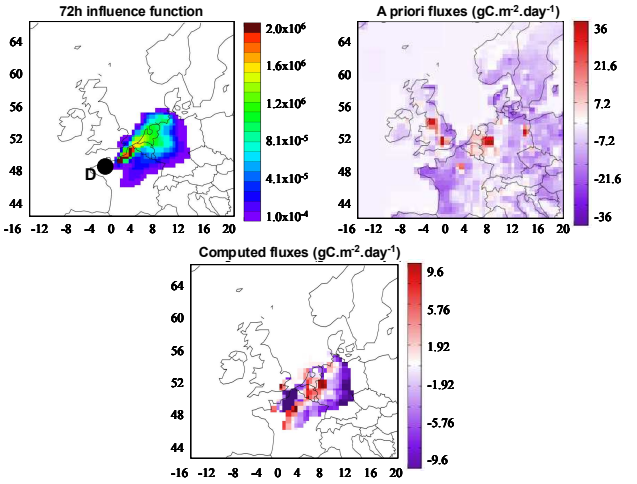

Fig. 8. Top left panel: LMDZt influence function (IF) calculated for 3 days backwards from the observing point (dark circle) corresponding to event D in Fig. 7a. Top right panel: a priori fluxes (anthropogenic, biospheric and oceanic), summed and averaged for the period from 21 May 2001, 12:00 UTC to 25 May 2001, 12:00 UTC. Low panel: Weighted fluxes contributing to the CO_2 signal recorded at the observing point. Flux units are in gC m^{-2} day^{-1}.

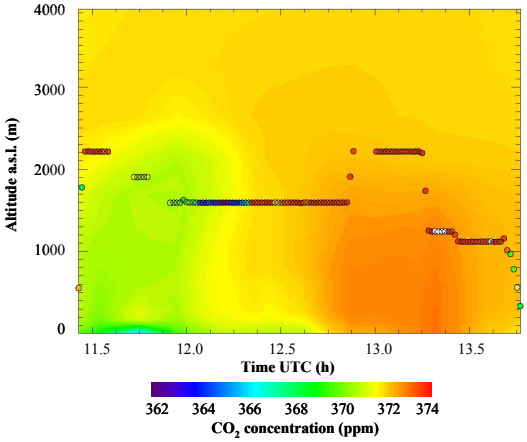

Fig. 9. Comparison of CO_2 concentration along the aircraft path on 25 May 2001 according to altitude and time (circles), with simulated CO_2 concentration fields from the LMDZt modeling framework. Note that the white color indicates high concentrations that are out of scale (∼380 ppm).

3.5 ppm from the model versus 11.5 ppm from observations, therefore the model framework underestimates extremes by a factor of 3 roughly.

So we conclude that the error on this method can be large for individual events and is more than 33% when considering averages.

3.3 Discussion

Both methods give a comparable CO_2 flux of the same order of magnitude within the Radon method uncertainty (35%), the error on the modeling method estimated to be at least 33%. This flux is the one seen at 1700 m, representative of the area over which the air masses travelled before reaching the observing point. The 5-days backward IF covers the North of France, The Benelux, The Netherlands, Germany, Western Poland and the Czech Republic. But most of the surface grid elements are concentrated over Northern France, Germany, The Benelux and Western Poland. The catchment area is of the order of 1500 km (longitudinally) per 700 km (latitudinally). This estimates the flux at this moment and for this region of Europe to be a net negative flux of −4.2 to −4.4 gC m^{-2} day^{-1}. The concordance between the ^{222}Rn method and the IF method relying on an explicit description of transport dynamics is encouraging. It suggests that, even if not optimized, the fluxes prescribed to LMDZt are rather realistic. In fact, the IF method can be applied to any observation point to estimate the footprint of the air mass before it reaches the measurement location. The flux scale is a function of the dynamical fields, of the time backwards and of the altitude of the observation point. The catchment area increases with altitude and can be defined using the IF maps (for example, for the profile done in the flat region of Brest, we get a fetch of 50×50 km^2 at 70 m a.s.l., 500×500 km^2 at 900 m of altitude and 1200×700 km^2 at 1500 m). Thus, the knowledge of IF should help to fill the gap between local and continental scale for carbon flux calculations on the continents. Of course, this paper only shows one case study and deeper studies must be conducted to better characterize the errors on the method, here estimated to be at least 33%. The use of optimized fluxes (from atmospheric inversions) and of mesoscale models for atmospheric transport may significantly reduce the uncertainties.

4 Conclusions

In this paper we have conducted a comparison between observations and modeling atmospheric CO_2 studies for the airborne CAATER campaigns that occured over Europe in May 2001 and October 2002, as described in the companion paper (Xueref-Remy et al., 2011).

Firstly, we compared CO_2 modeled and observed vertical profiles using different combinations of transport models (the global model LMDZt and the mesoscale model CHIMERE) and biospheric flux models with a CO_2 diurnal cycle (CASA, SiB2 and ORCHIDEE). For the CAATER-1 campaign, the observed mid-ABL gradient of CO_2 is not reproduced by any of the tested model combinations (LMDZt-CASA, LMDZt-SiB, LMDZt-ORCHIDEE and CHIMERE-ORCHIDEE), all being too diffusive. For the CAATER-2 campaign, CHIMERE-ORCHIDEE is closer to observations concerning the jump in CO_2 concentration between

the ABL and the FT, but the profile structure is better reproduced by LMDZt-CASA. However LMDZt is still too diffusive and the ABL height is not well located. On the whole, we can conclude that: (1) NEE fluxes sometimes play a role in the gradient magnitude and shape, the ORCHIDEE model (a climate driven model) giving the best results compared to SiB2 and CASA (process-based models); (2) however, mismatches between observed and modeled profiles mainly come from errors in the transport models. In fact, LMDZt systematically simulates vertical profiles that are too stiff, overestimating the mixing rate of the ABL into the FT. This conclusion was also given by Stephens et al. (2007) who reported a systematic overestimation of simulated vertical transport in Summer by 12 models from the TRANSCOM 3 Level 2 study (Gurney et al., 2004). During CAATER 2, the ABL height is generally too high in that model. The CHIMERE mesoscale model gives better results on average, as the vertical transport is less diffusive and the jumps are better reproduced. However CHIMERE is sometimes too variable, leading to incoherent structures. On the whole, the mesoscale model in this case study seems better than the global one in reproducing vertical profiles. Finally, this work highlights the fact that more intensive and regular vertical profiles are needed in the future to conduct further comparisons between observations and models, and thus to make important progress in the parameterization of the models.

Further, we coupled influence functions (IF) and CO_2 map fluxes to compute the CO_2 flux observed at a given point. We compared the results of this modeling method to CO_2 flux calculated with the Radon method from simultaneous CO_2 and Radon 222 measurements. Both methods were applied to a CAATER-1 campaign case study, during which a good correlation between in situ CO_2 measurements and semi-continuous Radon 222 observations was observed. Using IF from LMDZt (for which synoptic transport is known to be quite reliable: see Patra et al., 2008) we estimated the catchment area of the observation point (located at 1700 m a.s.l.) to be 1500 km (longitudinally) by 700 km (latitudinally) over Northern France, Benelux, Germany and Western Poland. Both methods give a CO_2 flux of the same order of magnitude (-4.2 to -4.4 gC m^{-2} day), within the uncertainty of the Radon method (35%), the uncertainty of the modeling method being estimated at more than 33%. The agreement between the results of both methods is very promising for future application of the modeling method on any observation point. However, errors in this second method need to be better assessed, for example at tall towers where simultaneous CO_2 and Radon 222 measurements can be conducted. Uncertainties may also be significantly reduced by using optimized fluxes (from atmospheric inversions) and mesoscale models for atmospheric transport.

Acknowledgements. This work was funded by the Institut National des Sciences de l'Univers, France, and by the European Commission in the framework of the AEROCARB project. We thank Dominique Filippi for providing the Radon data. We acknowledge Ingeborg Levin and Martina Schmidt for helpful discussions on the Radon calculations. The authors are very grateful to Nicolas Viovy for providing ORCHIDEE fluxes. We thank very much Mary Minnock for text corrections.

Edited by: J. Rinne

The publication of this article is financed by CNRS-INSU.

References

Andres, R. J., Marland, G., Fung, I., and Matthews E.: A 1°×1° distribution of carbon dioxide emissions from fossil fuel consumption and cement manufacture – 1950–1990, Global Biogeochem. Cy., 10, 419–429,1996.

Biraud, S., Ciais, P., Ramonet, M., Simmonds, P., Kazan, V., Monfray, P., Spain, T. G., and Jennings, S. G.: European greenhouse gas emissions estimates from continuous atmospheric measurements at Mace Head, Ireland, J. Geophys. Res., 105(D1), 1351–1366, 2000.

Biraud, S., Ciais, P., Ramonet, M., Simmonds, P., Kazan, V., Monfray, P., O'Doherty, S., Spain, G., and Jennings, S. G.: Quantification of carbon dioxide, methane, nitrous oxide and chloroform emissions over Ireland from atmospheric observations at Mace Head, Tellus, 54B, 41–60, 2002.

Bousquet P., Ciais, P., Peylin, P., Ramonet, M., and Monfray, P.: Inverse modeling of annual atmospheric CO_2 sources and sinks: 1 – Method and control inversion, J. Geophys. Res., 104(D21), 26161–26178, 1999.

Eckhardt, K.: Messung des Radonflusses und seiner Abhängigkeit von der Bodenbeschaffenheit, Universität Heidelberg, Heidelberg, 1990.

Filiberti, P., Friedlingstein, P., Grandpeix, J. Y., Krinner, G., Levan, P., Li, Z. X., and Lott, F.: The LMDZ4 general circulation model: climate performance and sensitivity to parametrized physics with emphasis on tropical convection, Clim. Dynam., 27, 787–813, 2006.

Filippi, D.: Etude et développement d'un instrument aéroporté destiné à la collecte des aérosols et à la mesure du Radon-222 par son dépot actif, phD, Université Paris-6, 2000.

Geels, C., Gloor, M., Ciais, P., Bousquet, P., Peylin, P., Vermeulen, A. T., Dargaville, R., Aalto, T., Brandt, J., Christensen, J. H., Frohn, L. M., Haszpra, L., Karstens, U., Rödenbeck, C., Ramonet, M., Carboni, G., and Santaguida, R.: Comparing atmospheric transport models for future regional inversions over Europe – Part 1: mapping the atmospheric CO2 signals, At-

mos. Chem. Phys., 7, 3461–3479, doi:10.5194/acp-7-3461-2007, 2007.

Gerbig, C., Lin, J. C., Wofsy, S. C., Daube, B. C., Andrews, A. E., Stephens, Bakwin, P. S., and Grainger, C. A.: Towards constraining regional-scale fluxes of CO_2 with atmospheric observations over a continent: 1. Observed Spatial Variability, J. Geophys. Res., 108, 4756, doi:10.1029/2002JD003018, 2003a.

Gerbig, C., Lin, J. C., Wofsy, S. C., Daube, B. C., Andrews, A. E., Stephens, B. B., Bakwin, P. S., and Grainger, C. A.: Toward constraining regional-scale fluxes of CO_2 with atmospheric observations over a continent: 2. Analysis of COBRA data using a receptor-oriented framework, J. Geophys. Res., 108(D24), 4757, doi:10.1029/2003JD003770, 2003b.

Gibert F., Schmidt, M., Cuesta, J., Larmanou, E., Ramonet, M., Flamant, P.H., Xueref, I., and Ciais, P.: Retrieval of average CO_2 fluxes by combining in-situ CO_2measurements and backscatter Lidar information, J. Geophys. Res., 112, D10301, doi:10.1029/2006JD008190, 2007.

GLOBALVIEW-CO2: Cooperative Atmospheric Data Integration Project – Carbon Dioxide, CD-ROM, NOAA GMD, Boulder, Colorado (Also available on Internet via anonymous FTP to ftp.cmdl.noaa.gov, Path: ccg/co2/GLOBALVIEW), 2006.

Gloor, M., Fan, S., Sarmiento, J., and Pacala, S.: Optimal sampling of the atmosphere for purpose of inverse modelling – a model study, Global Biogeochem. Cy., 14(1), 407-428, 2000.

Gloor, M., Bakwin, P., Hurst, D., Lock, L., Draxler, R., and Tans, P.: What is the concentration footprint of a tall tower?, J. Geophys. Res., 106(D16), 17831–17840, 2001.

Grell, G. A., Dudhia, J., and Stauffer, D. R.: A description of the fifth generation of Penn State/NCAR mesoscale model (MM5), NCAR Technical Note, NCAR/TN-398+STR, 117 pp., available at: http://www.mmm.ucar.edu/mm5/doc1.html, 1994.

Gurney, K. R., Law, R., Denning, A. S., et al.: Towards robust regional estimates of CO_2 sources and sinks using atmospheric transport models, Nature, 415, 626–630, 2002.

Gurney, K. R., Law, R. M., Denning, A. S., et al.: Transcom 3 inversion intercomparison: Model mean results for the estimation of seasonal carbon sources and sinks, Global Biocheochem. Cy., 18, GB1010, doi:10.1029/2003GB002111, 2004.

Haszpra, L., Barcza, Z., Davis, K. J., and Tarczay, K.: Long-term tall tower carbon dioxide flux monitoring over an area of mixed vegetation, Agr. Forest Meteorol., 132(1–2), 58–77, 2005.

Hauglustaine, D. A., Hourdin, F., Jourdain, L., Filiberti, M.-A., Walters, S., Lamarque, J.-F., and Holland, E. A.: Interactive chemistry in the Laboratoire de Meteorologie Dynamique general circulation model – Description and background tropospheric chemistry evaluation, J. Geophys. Res., 109, 4314, doi:10.1029/2003JD003957, 2004.

Hourdin, F. and Armengaud, A.: Test of a hierarchy of finite-volume schemes for transport of trace species in an atmospheric general circulation model, Mon. Weather Rev., 127, 822–837, 1999.

Hourdin, F. D., Couvreux, F., and Menut, L.: Parameterization of the dry convective boundary layer based on a mass flux representation of thermals, J. Atmos. Sci., 59(6), 1105–1123, 2002.

Hourdin, F., Musat, I., Bony, S., Braconnot, P., Codron, F., Dufresne, J. L., Fairhead, L., le Filiberti, M. A., Friedlingstein, P., Grandpeix, J. Y., Krinner, G., LeVan, P., Li, Z. X., and Lott, F.: The LMDZ4 general circulation model: climate performance and sensitivity to parametrized physics with emphasis on tropical convection, Clim. Dynam., 27, 787–813, doi:10.1007/s00382-006-0158-0, 2006.

Ielsch, G., Ferry, C., Tymen, G., and Robe, M. C.: Study of a predictive methodology for quantification and mapping of the radon-222 exhaltation rate, J. Environ. Radioactiv., 63, 15–33, 2002.

Jutzi, S.: Verteilung der Boden 222Rn exhalation in Europa, thesis, Inst. für Umweltphys., Univ. of Heidelberg, Heidelberg, Germany, 2001.

Krinner, G., Viovy, De Noblet-Ducoudré, N., Ogée, J., Polcher, J., Friedlingstein, P., Ciais, P., Sitch, S., and Prentice, I. C.: A dynamic global vegetation model for studies of the coupled atmosphere-biosphere system, Global Biogeochem. Cy., 19, GB1015, doi:10.1029/2003GB002199, 2005.

Kritz, M. A. and Rosner, S. W.: Validation of an off-line three-dimentional chemical transport model using observed radon profiles, J. Geophys. Res., 103(D7), 8425–8432, 1998.

Krol, M.: A First Attempt to use Variability at Synoptical Time Scales in Constraining Trace gas Emissions, Eos Trans. AGU, 84(46), Fall Meet. Suppl., Abstract A51B-03, 2003.

Lauvaux, T., Gioli, B., Sarrat, C., Rayner, P. J., Ciais, P., Chevallier, F., Noilhan, J., Miglietta, F., Brunet, Y., Ceschia, E., Dolman, H., Elbers, J. A., Gerbig, C., Hutjes, R., Jarosz, N., Legain, D., and Uliasz, M.: Bridging the gap between atmospheric concentrations and local ecosystem measurements, Geophys.Res. Lett., 36, L19809, doi:10.1029/2009GL039574, 2009.

Law, R.M., Peters, W., Rodenbeck, C., and TRANSCOM contributors: TransCom model simulations of hourly atmospheric CO_2: experimental overview and diurnal cycle results for 2002, Global Biogeochem. Cy., 22, GB3009, doi:10.1029/2007GB003050, 2007.

Levin, I.: Atmosphärisches CO_2, Quellen und Senken auf dem Europäischen Kontinent, Ph.D. thesis, Univ. of heidelberg, Heidelberg, Germany, 1984.

Levin, I., Glatzel-Mattheier, H., Marik, T., Cuntz, M., Schmidt, M., and Worthy, D. E.: Verification of German methane emission inventories and their recent changes based on atmospheric observations, J. Geophys. Res., 104(D3), 3447–3456, 1999.

Nazaroff: Radon transport from soil to air, Rev. Geophys., 30(2), 137–160, 1992.

Peylin, P., Rayner, P. J., Bousquet, P., Carouge, C., Hourdin, F., Heinrich, P., Ciais, P., and AEROCARB contributors: Daily CO_2 flux estimates over Europe from continuous atmospheric measurements: 1, inverse methodology, Atmos. Chem. Phys., 5, 3173–3186, doi:10.5194/acp-5-3173-2005, 2005.

Patra, P. K., Law, R. M., Peters, W., Rödenbeck, C., Takigawa, M., Aulagnier, C., Baker, I., Bergmann, D. J., Bousquet, P., Brandt, J., Bruhwiler, L., Cameron-Smith, P. J., Christensen, J. H., Delage, F., Denning, A. S., Fan, S., Geels, C., Houweling, S., Imasu, R., Karstens, U., Kawa, S. R., Kleist, J., Krol, M. C., Lin, S. J., Lokupitiya, R., Maki, T., Maksyutov, S., Niwa, Y., Onishi, R., Parazoo, N., Pieterse, G., Rivier, L., Satoh, M., Serrar, S., Taguchi, S., Vautard, R., Vermeulen, A., and Zhu, Z.: TransCom model simulations of hourly atmospheric CO_2: Analysis of synoptic-scale variations for the period 2002–2003, Global Biogeochem. Cy., 22, GB4013, doi:10.1029/2007GB003081, 2008.

Peylin, P., Houweling, S., Krol, M. C., Karstens, U., Rödenbeck, C., Geels, C., Vermeulen, A., Badawy, B., Aulagnier, C., Pregger, T., Delage, F., Pieterse, G., Ciais, P., and Heimann, M.: Importance

of fossil fuel emission uncertainties over Europe for CO_2 modeling: model intercomparison, Atmos. Chem. Phys. Discuss., 9, 7457–7503, doi:10.5194/acpd-9-7457-2009, 2009.

Pregger, T., Scholz, Y., and Friedrich, R.: Documentation of the anthropogenic GHG emission data for Europe provided in the Frame of CarboEurope GHG and CarboEurope IP, Project report, Institut für Energiewirtschaft und Rationelle Energieanwendung, Universität Stuttgart, 5 Stuttgart, Germany, 7463–7464 and p. 7487, 2007.

Ramonet, M., Ciais, P., Nepomniachii, I., Sidorov, K., Neubert, R. E. M., Langendörfer, U., Picard, D., Kazan, V., Biraud, S., Gusti, M., Kolle, O., Schulze, E. D., and Lloyd, J.: Three years of aircraft-based trace gas measurements over the Fyodorovskoye southern taiga forest, 300 km north-west of Moscow, Tellus, 54B, 713–734, 2002.

Randerson, J. T., Thompson, M. V., Conway, T. J., Fung, I. Y., and Field, C. B.: The contribution of terrestrial sources and sinks to trends in the seasonal cycle of atmospheric carbon dioxide, Global Biogeochem. Cy., 11, 535–560, 1997.

Rödenbeck, C., Houweling, S., Gloor, M., and Heimann, M.: CO_2 flux history 1982–2001 inferred from atmospheric data using a global inversion of atmospheric transport, Atmos. Chem. Phys., 3, 1919–1964, doi:10.5194/acp-3-1919-2003, 2003.

Sarrat, C., Noilhan, J., Lacarrere, P., Donier, S., Dolman, H., Gerbig, C., Ciais, P., and Butet, A.: Atmospheric CO_2 modeling at the regional scale: Application to the CarboEurope Regional Experiment, J. Geophys. Res., 112, D12105, doi:10.1029/2006JD008107, 2007.

Schmidt, H., Derognat, C., Vautard, R., and Beekmann, M.: A comparison of simulated and observed ozone mixing ratios for the summer of 1998 in Western Europe, Atmos. Environ., 36, 6277–6297, 2001.

Schmidt, M., Graul, R., Sartorius, H., and Levin, I.: Carbon dioxide and methane in continental Europe: a climatology, and ^{222}Radon-based emission estimates, Tellus B, 48(4), 457–473, 1996.

Schmidt, M., Glatzel-Mattheier, H., Sartorius, H., Worthy, D. E., and Levin, I.: Western European N_2O emissions: A top-down approach based on atmospheric observations, J. Geophys. Res., 106(D6), 5507–5516, 2001.

Schmidt, M., Graul, R., Sartorius, H., and Levin, I.: The Schauinsland CO_2 record: 30 years of continental observations and their implications for the variability of the European CO_2 budget, J. Geophys. Res., 108(D19), 4619–4626, 2003.

Sellers, P. J., Los, S. O., Tucker, J., Justice, C. O., Dazlich, D. A., Collatz, J. A., and Randall, D. R.: A revised land-surface parameterization (SiB2) for atmospheric GCMs: Part 2: The generation of global fields of terrestrial biophysical parameters from satellite data, J. Climate, 9, 706–737, 1996.

Stephens, B. B., Gurney, K. R., Tans, P. P., Sweeney, C., Peters, W., Bruhwiler, L., Ciais, P., Ramonet, M., Bousquet, P., Nakazawa, T., Aoki, S., Machida, T., Inoue, G., Vinnichenko, N., Lloyd, J., Jordan, A., Heimann, M., Shibistova, O., Langenfelds, R. L., Steele, L. P., Francey, R. J., and Denning, A. S.: Weak Northern and Strong Tropical Land Carbon Uptake from Vertical Profiles of Atmospheric CO_2, Science, 316(5832), 1732–1735, doi:10.1126/science.1137004, 2007.

Stohl, A. and Koffi, N. E.: Evaluation of trajectories calculated from ECMWF data against constant volume balloon flights during ETEX, Atmos. Environ., 32, 4151–4156, 1998a.

Stohl, A., Hittenberger, M., and Wotawa, G.: Validation of the Lagrangian particle dispersion model FLEXPART against large scale tracer experiments, Atmos. Environ., 32, 4245–4264, 1998b.

Stohl, A. and Seibert, P.: Accuracy of trajectories as determined from the conservation of meteorological tracers, Q. J. Roy. Meteorol. Soc., 124, 1465–1484, 1998c.

Szegvary, T., Leuenberger, M. C., and Conen, F.: Predicting terrestrial ^{222}Rn flux using gamma dose rate as a proxy, Atmos. Chem. Phys., 7, 2789–2795, doi:10.5194/acp-7-2789-2007, 2007.

Takahashi, T., Wanninkhof, R. H., Feely, R. A., Weiss, R. F., Chipman, D. W., Bates, N., Olafsson, J., Sabine, C., and Sutherland, S. C.: Net sea-air CO_2 flux over the global oceans: An improved estimate based on the air-sea pCO_2 difference, in 2nd CO_2 in ocean symposium, Tsukuba, Japan, January 18–23, 1999.

Takahashi, T., Sutherland, S. C., Sweeney, C., Poisson, A., Metzl, A., et al.: Global Sea-Air CO_2 Flux Based on Climatological Surface Ocean pCO_2, and Seasonal Biological and Temperature Effect, Deep Sea Res. II, 49(9–10), 1601–1622, 2002.

Uppala, S. M., Kållberg, P. W., Simmons, A. J., Andrae, U., da Costa Bechtold, V., Fiorino, M., Gibson, J. K., Haseler, J., Hernandez, A., Kelly, G. A., Li, X., Onogi, K., Saarinen, S., Sokka, N., Allan, R. P., Andersson, E., Arpe, K., Balmaseda, M. A., Beljaars, A. C. M., van de Berg, L., Bidlot, J., Bormann, N., Caires, S., Chevallier, F., Dethof, A., Dragosavac, M., Fisher, M., Fuentes, M., Hagemann, S., Hólm, E., Hoskins, B. J., Isaksen, L., Janssen, P. A. E. M., Jenne, R., McNally, A. P., Mahfouf, J.-F., Morcrette, J.-J., Rayner, N. A., Saunders, R. W., Simon, P., Sterl, A., Trenberth, K. E., Untch, A., Vasiljevic, D., Viterbo, P., and Woollen, J.: The ERA-40 re-analysis, Q. J. Roy. Meteorol. Soc., 131, 2961–3012, doi:10.1256/qj.04.176, 2005.

Wilson, S. R., Dick, A. L., Fraser, P. J., and Whittlestone, S.: Nitrous oxide estimates for south-eastern Australia, J. Atmos. Chem., 26, 169–188, 1997.

Yi, C., Davis, K. J., Bakwin, P. S., Denning, A. S., Zhang, N., Desai, A., Lin, J. C., and Gerbig, C.: Observed covariance between ecosystem carbon exchange and atmospheric boundary layer dynamics at a site in northern Wisconsin, J. Geophys. Res., 109, D08302, doi:10.1029/2003JD004164, 2004.

Xueref-Remy, I., Messager, C., Filippi, D., Pastel, M., Nedelec, P., Ramonet, M., Paris, J. D., and Ciais, P.: Variability and budget of CO_2 in Europe: analysis of the CAATER airborne campaigns – Part 1: Observed variability, Atmos. Chem. Phys., 11, 5655–5672, doi:10.5194/acp-11-5655-2011, 2011.